

Measurements of the Branching Fractions and Bounds on the Charge Asymmetries of Charmless Three-Body Charged B Decays

B. Aubert,¹ R. Barate,¹ D. Boutigny,¹ J.-M. Gaillard,¹ A. Hicheur,¹ Y. Karyotakis,¹ J. P. Lees,¹ P. Robbe,¹ V. Tisserand,¹ A. Zghiche,¹ A. Palano,² A. Pompili,² J. C. Chen,³ N. D. Qi,³ G. Rong,³ P. Wang,³ Y. S. Zhu,³ G. Eigen,⁴ I. Ofte,⁴ B. Stugu,⁴ G. S. Abrams,⁵ A. W. Borgland,⁵ A. B. Breon,⁵ D. N. Brown,⁵ J. Button-Shafer,⁵ R. N. Cahn,⁵ E. Charles,⁵ C. T. Day,⁵ M. S. Gill,⁵ A. V. Gritsan,⁵ Y. Groysman,⁵ R. G. Jacobsen,⁵ R. W. Kadel,⁵ J. Kadyk,⁵ L. T. Kerth,⁵ Yu. G. Kolomensky,⁵ J. F. Kral,⁵ G. Kukartsev,⁵ C. LeClerc,⁵ M. E. Levi,⁵ G. Lynch,⁵ L. M. Mir,⁵ P. J. Oddone,⁵ T. J. Orimoto,⁵ M. Pripstein,⁵ N. A. Roe,⁵ A. Romosan,⁵ M. T. Ronan,⁵ V. G. Shelkov,⁵ A. V. Telnov,⁵ W. A. Wenzel,⁵ T. J. Harrison,⁶ C. M. Hawkes,⁶ D. J. Knowles,⁶ R. C. Penny,⁶ A. T. Watson,⁶ N. K. Watson,⁶ T. Deppermann,⁷ K. Goetzen,⁷ H. Koch,⁷ B. Lewandowski,⁷ M. Pelizaeus,⁷ K. Peters,⁷ H. Schmuecker,⁷ M. Steinke,⁷ N. R. Barlow,⁸ W. Bhimji,⁸ J. T. Boyd,⁸ N. Chevalier,⁸ W. N. Cottingham,⁸ C. Mackay,⁸ F. F. Wilson,⁸ C. Hearty,⁹ T. S. Mattison,⁹ J. A. McKenna,⁹ D. Thiessen,⁹ P. Kyberd,¹⁰ A. K. McKemey,¹⁰ V. E. Blinov,¹¹ A. D. Bukan,¹¹ V. B. Golubev,¹¹ V. N. Ivanchenko,¹¹ E. A. Kravchenko,¹¹ A. P. Onuchin,¹¹ S. I. Serednyakov,¹¹ Yu. I. Skovpen,¹¹ E. P. Solodov,¹¹ A. N. Yushkov,¹¹ D. Best,¹² M. Chao,¹² D. Kirkby,¹² A. J. Lankford,¹² M. Mandelkern,¹² S. McMahon,¹² R. K. Mommsen,¹² W. Roethel,¹² D. P. Stoker,¹² C. Buchanan,¹³ H. K. Hadavand,¹⁴ E. J. Hill,¹⁴ D. B. MacFarlane,¹⁴ H. P. Paar,¹⁴ Sh. Rahatlou,¹⁴ U. Schwanke,¹⁴ V. Sharma,¹⁴ J. W. Berryhill,¹⁵ C. Campagnari,¹⁵ B. Dahmes,¹⁵ N. Kuznetsova,¹⁵ S. L. Levy,¹⁵ O. Long,¹⁵ A. Lu,¹⁵ M. A. Mazur,¹⁵ J. D. Richman,¹⁵ W. Verkerke,¹⁵ J. Beringer,¹⁶ A. M. Eisner,¹⁶ C. A. Heusch,¹⁶ W. S. Lockman,¹⁶ T. Schalk,¹⁶ R. E. Schmitz,¹⁶ B. A. Schumm,¹⁶ A. Seiden,¹⁶ M. Turri,¹⁶ W. Walkowiak,¹⁶ D. C. Williams,¹⁶ M. G. Wilson,¹⁶ J. Albert,¹⁷ E. Chen,¹⁷ M. P. Dorsten,¹⁷ G. P. Dubois-Felsmann,¹⁷ A. Dvoretskii,¹⁷ D. G. Hitlin,¹⁷ I. Narsky,¹⁷ F. C. Porter,¹⁷ A. Ryd,¹⁷ A. Samuel,¹⁷ S. Yang,¹⁷ S. Jayatilleke,¹⁸ G. Mancinelli,¹⁸ B. T. Meadows,¹⁸ M. D. Sokoloff,¹⁸ T. Barillari,¹⁹ F. Blanc,¹⁹ P. Bloom,¹⁹ P. J. Clark,¹⁹ W. T. Ford,¹⁹ U. Nauenberg,¹⁹ A. Olivas,¹⁹ P. Rankin,¹⁹ J. Roy,¹⁹ J. G. Smith,¹⁹ W. C. van Hoek,¹⁹ L. Zhang,¹⁹ J. L. Harton,²⁰ T. Hu,²⁰ A. Soffer,²⁰ W. H. Toki,²⁰ R. J. Wilson,²⁰ J. Zhang,²⁰ D. Altenburg,²¹ T. Brandt,²¹ J. Brose,²¹ T. Colberg,²¹ M. Dickopp,²¹ R. S. Dubitzky,²¹ A. Hauke,²¹ H. M. Lacker,²¹ E. Maly,²¹ R. Müller-Pfefferkorn,²¹ R. Nogowski,²¹ S. Otto,²¹ K. R. Schubert,²¹ R. Schwierz,²¹ B. Spaan,²¹ L. Wilden,²¹ D. Bernard,²² G. R. Bonneau,²² F. Brochard,²² J. Cohen-Tanugi,²² Ch. Thiebaut,²² G. Vasileiadis,²² M. Verderi,²² A. Khan,²³ D. Lavin,²³ F. Muheim,²³ S. Playfer,²³ J. E. Swain,²³ J. Tinslay,²³ C. Bozzi,²⁴ L. Piemontese,²⁴ A. Sarti,²⁴ E. Treadwell,²⁵ F. Anulli,^{26,*} R. Baldini-Ferroli,²⁶ A. Calcaterra,²⁶ R. de Sangro,²⁶ D. Falciai,²⁶ G. Finocchiaro,²⁶ P. Patteri,²⁶ I. M. Peruzzi,^{26,*} M. Piccolo,²⁶ A. Zallo,²⁶ A. Buzzo,²⁷ R. Contri,²⁷ G. Crosetti,²⁷ M. Lo Vetere,²⁷ M. Macri,²⁷ M. R. Monge,²⁷ S. Passaggio,²⁷ F. C. Pastore,²⁷ C. Patrignani,²⁷ E. Robutti,²⁷ A. Santroni,²⁷ S. Tosi,²⁷ S. Bailey,²⁸ M. Morii,²⁸ G. J. Grenier,²⁹ S.-J. Lee,²⁹ U. Mallik,²⁹ J. Cochran,³⁰ H. B. Crawley,³⁰ J. Lamsa,³⁰ W. T. Meyer,³⁰ S. Prell,³⁰ E. I. Rosenberg,³⁰ J. Yi,³⁰ M. Davier,³¹ G. Grosdidier,³¹ A. Höcker,³¹ S. Laplace,³¹ F. Le Diberder,³¹ V. Lepeltier,³¹ A. M. Lutz,³¹ T. C. Petersen,³¹ S. Plaszczynski,³¹ M. H. Schune,³¹ L. Tantot,³¹ G. Wormser,³¹ R. M. Bionta,³² V. Briglijević,³² C. H. Cheng,³² D. J. Lange,³² D. M. Wright,³² A. J. Bevan,³³ J. R. Fry,³³ E. Gabathuler,³³ R. Gamet,³³ M. Kay,³³ D. J. Payne,³³ R. J. Sloane,³³ C. Touramanis,³³ M. L. Aspinwall,³⁴ D. A. Bowerman,³⁴ P. D. Dauncey,³⁴ U. Egede,³⁴ I. Eschrich,³⁴ G. W. Morton,³⁴ J. A. Nash,³⁴ P. Sanders,³⁴ G. P. Taylor,³⁴ J. J. Back,³⁵ G. Bellodi,³⁵ P. F. Harrison,³⁵ H. W. Shorthouse,³⁵ P. Strother,³⁵ P. B. Vidal,³⁵ G. Cowan,³⁶ H. U. Flaecher,³⁶ S. George,³⁶ M. G. Green,³⁶ A. Kurup,³⁶ C. E. Marker,³⁶ T. R. McMahon,³⁶ S. Ricciardi,³⁶ F. Salvatore,³⁶ G. Vaitsas,³⁶ M. A. Winter,³⁶ D. Brown,³⁷ C. L. Davis,³⁷ J. Allison,³⁸ R. J. Barlow,³⁸ A. C. Forti,³⁸ P. A. Hart,³⁸ F. Jackson,³⁸ G. D. Lafferty,³⁸ A. J. Lyon,³⁸ J. H. Weatherall,³⁸ J. C. Williams,³⁸ A. Farbin,³⁹ A. Jawahery,³⁹ D. Kovalskyi,³⁹ C. K. Lae,³⁹ V. Lillard,³⁹ D. A. Roberts,³⁹ G. Blaylock,⁴⁰ C. Dallapiccola,⁴⁰ K. T. Flood,⁴⁰ S. S. Hertzbach,⁴⁰ R. Kofler,⁴⁰ V. B. Koptchev,⁴⁰ T. B. Moore,⁴⁰ H. Staengle,⁴⁰ S. Willocq,⁴⁰ R. Cowan,⁴¹ G. Sciolla,⁴¹ F. Taylor,⁴¹ R. K. Yamamoto,⁴¹ D. J. J. Mangeol,⁴² M. Milek,⁴² P. M. Patel,⁴² A. Lazzaro,⁴³ F. Palombo,⁴³ J. M. Bauer,⁴⁴ L. Cremaldi,⁴⁴ V. Eschenburg,⁴⁴ R. Godang,⁴⁴ R. Kroeger,⁴⁴ J. Reidy,⁴⁴

D. A. Sanders,⁴⁴ D. J. Summers,⁴⁴ H. W. Zhao,⁴⁴ C. Hast,⁴⁵ P. Taras,⁴⁵ H. Nicholson,⁴⁶ C. Cartaro,⁴⁷ N. Cavallo,⁴⁷ G. De Nardo,⁴⁷ F. Fabozzi,⁴⁷, † C. Gatto,⁴⁷ L. Lista,⁴⁷ P. Paolucci,⁴⁷ D. Piccolo,⁴⁷ C. Sciacca,⁴⁷ M. A. Baak,⁴⁸ G. Raven,⁴⁸ J. M. LoSecco,⁴⁹ T. A. Gabriel,⁵⁰ B. Brau,⁵¹ T. Pulliam,⁵¹ J. Brau,⁵² R. Frey,⁵² M. Iwasaki,⁵² C. T. Potter,⁵² N. B. Sinev,⁵² D. Strom,⁵² E. Torrence,⁵² F. Colecchia,⁵³ A. Dorigo,⁵³ F. Galeazzi,⁵³ M. Margoni,⁵³ M. Morandin,⁵³ M. Posocco,⁵³ M. Rotondo,⁵³ F. Simonetto,⁵³ R. Stroili,⁵³ G. Tiozzo,⁵³ C. Voci,⁵³ M. Benayoun,⁵⁴ H. Briand,⁵⁴ J. Chauveau,⁵⁴ P. David,⁵⁴ Ch. de la Vaissière,⁵⁴ L. Del Buono,⁵⁴ O. Hamon,⁵⁴ Ph. Leruste,⁵⁴ J. Ocariz,⁵⁴ M. Pivk,⁵⁴ L. Roos,⁵⁴ J. Stark,⁵⁴ S. T'Jampens,⁵⁴ P. F. Manfredi,⁵⁵ V. Re,⁵⁵ L. Gladney,⁵⁶ Q. H. Guo,⁵⁶ J. Panetta,⁵⁶ C. Angelini,⁵⁷ G. Batignani,⁵⁷ S. Bettarini,⁵⁷ M. Bondioli,⁵⁷ F. Bucci,⁵⁷ G. Calderini,⁵⁷ M. Carpinelli,⁵⁷ F. Forti,⁵⁷ M. A. Giorgi,⁵⁷ A. Lusiani,⁵⁷ G. Marchiori,⁵⁷ F. Martinez-Vidal,⁵⁷, † M. Morganti,⁵⁷ N. Neri,⁵⁷ E. Paoloni,⁵⁷ M. Rama,⁵⁷ G. Rizzo,⁵⁷ F. Sandrelli,⁵⁷ J. Walsh,⁵⁷ M. Haire,⁵⁸ D. Judd,⁵⁸ K. Paick,⁵⁸ D. E. Wagoner,⁵⁸ N. Danielson,⁵⁹ P. Elmer,⁵⁹ C. Lu,⁵⁹ V. Miftakov,⁵⁹ J. Olsen,⁵⁹ A. J. S. Smith,⁵⁹ E. W. Varnes,⁵⁹ F. Bellini,⁶⁰ G. Cavoto,^{59,60} D. del Re,⁶⁰ R. Faccini,^{14,60} F. Ferrarotto,⁶⁰ F. Ferroni,⁶⁰ M. Gaspero,⁶⁰ E. Leonardi,⁶⁰ M. A. Mazzoni,⁶⁰ S. Morganti,⁶⁰ M. Pierini,⁶⁰ G. Piredda,⁶⁰ F. Safai Tehrani,⁶⁰ M. Serra,⁶⁰ C. Voena,⁶⁰ S. Christ,⁶¹ G. Wagner,⁶¹ R. Waldi,⁶¹ T. Adye,⁶² N. De Groot,⁶² B. Franek,⁶² N. I. Geddes,⁶² G. P. Gopal,⁶² E. O. Olaiya,⁶² S. M. Xella,⁶² R. Aleksan,⁶³ S. Emery,⁶³ A. Gaidot,⁶³ S. F. Ganzhur,⁶³ P.-F. Giraud,⁶³ G. Hamel de Monchenault,⁶³ W. Kozanecki,⁶³ M. Langer,⁶³ G. W. London,⁶³ B. Mayer,⁶³ G. Schott,⁶³ G. Vasseur,⁶³ Ch. Yecho,⁶³ M. Zito,⁶³ M. V. Purohit,⁶⁴ A. W. Weidemann,⁶⁴ F. X. Yumiceva,⁶⁴ D. Aston,⁶⁵ R. Bartoldus,⁶⁵ N. Berger,⁶⁵ A. M. Boyarski,⁶⁵ O. L. Buchmueller,⁶⁵ M. R. Convery,⁶⁵ D. P. Coupal,⁶⁵ D. Dong,⁶⁵ J. Dorfan,⁶⁵ D. Dujmic,⁶⁵ W. Dunwoodie,⁶⁵ R. C. Field,⁶⁵ T. Glanzman,⁶⁵ S. J. Gowdy,⁶⁵ E. Grauges-Pous,⁶⁵ T. Hadig,⁶⁵ V. Halyo,⁶⁵ T. Hryna'ova,⁶⁵ W. R. Innes,⁶⁵ C. P. Jessop,⁶⁵ M. H. Kelsey,⁶⁵ P. Kim,⁶⁵ M. L. Kocian,⁶⁵ U. Langenegger,⁶⁵ D. W. G. S. Leith,⁶⁵ S. Luitz,⁶⁵ V. Luth,⁶⁵ H. L. Lynch,⁶⁵ H. Marsiske,⁶⁵ S. Menke,⁶⁵ R. Messner,⁶⁵ D. R. Muller,⁶⁵ C. P. O'Grady,⁶⁵ V. E. Ozcan,⁶⁵ A. Perazzo,⁶⁵ M. Perl,⁶⁵ S. Petrak,⁶⁵ B. N. Ratcliff,⁶⁵ S. H. Robertson,⁶⁵ A. Roodman,⁶⁵ A. A. Salnikov,⁶⁵ R. H. Schindler,⁶⁵ J. Schwiening,⁶⁵ G. Simi,⁶⁵ A. Snyder,⁶⁵ A. Soha,⁶⁵ J. Stelzer,⁶⁵ D. Su,⁶⁵ M. K. Sullivan,⁶⁵ H. A. Tanaka,⁶⁵ J. Va'vra,⁶⁵ S. R. Wagner,⁶⁵ M. Weaver,⁶⁵ A. J. R. Weinstein,⁶⁵ W. J. Wisniewski,⁶⁵ D. H. Wright,⁶⁵ C. C. Young,⁶⁵ P. R. Burchat,⁶⁶ T. I. Meyer,⁶⁶ C. Roat,⁶⁶ S. Ahmed,⁶⁷ J. A. Ernst,⁶⁷ W. Bugg,⁶⁸ M. Krishnamurthy,⁶⁸ S. M. Spanier,⁶⁸ R. Eckmann,⁶⁹ H. Kim,⁶⁹ J. L. Ritchie,⁶⁹ R. F. Schwitters,⁶⁹ J. M. Izen,⁷⁰ I. Kitayama,⁷⁰ X. C. Lou,⁷⁰ S. Ye,⁷⁰ F. Bianchi,⁷¹ M. Bona,⁷¹ F. Gallo,⁷¹ D. Gamba,⁷¹ C. Borean,⁷² L. Bosisio,⁷² G. Della Ricca,⁷² S. Dittongo,⁷² S. Grancagnolo,⁷² L. Lanceri,⁷² P. Poropat,⁷², ‡ L. Vitale,⁷² G. Vuagnin,⁷² R. S. Pavanini,⁷³ Sw. Banerjee,⁷⁴ C. M. Brown,⁷⁴ D. Fortin,⁷⁴ P. D. Jackson,⁷⁴ R. Kowalewski,⁷⁴ J. M. Roney,⁷⁴ H. R. Band,⁷⁵ S. Dasu,⁷⁵ M. Datta,⁷⁵ A. M. Eichenbaum,⁷⁵ H. Hu,⁷⁵ J. R. Johnson,⁷⁵ R. Liu,⁷⁵ F. Di Lodovico,⁷⁵ A. K. Mohapatra,⁷⁵ Y. Pan,⁷⁵ R. Prepost,⁷⁵ S. J. Sekula,⁷⁵ J. H. von Wimmersperg-Toeller,⁷⁵ J. Wu,⁷⁵ S. L. Wu,⁷⁵ Z. Yu,⁷⁵ and H. Neal⁷⁶

(The BABAR Collaboration)

¹Laboratoire de Physique des Particules, F-74941 Annecy-le-Vieux, France

²Università di Bari, Dipartimento di Fisica and INFN, I-70126 Bari, Italy

³Institute of High Energy Physics, Beijing 100039, China

⁴University of Bergen, Inst. of Physics, N-5007 Bergen, Norway

⁵Lawrence Berkeley National Laboratory and University of California, Berkeley, CA 94720, USA

⁶University of Birmingham, Birmingham, B15 2TT, United Kingdom

⁷Ruhr Universität Bochum, Institut für Experimentalphysik 1, D-44780 Bochum, Germany

⁸University of Bristol, Bristol BS8 1TL, United Kingdom

⁹University of British Columbia, Vancouver, BC, Canada V6T 1Z1

¹⁰Brunel University, Uxbridge, Middlesex UB8 3PH, United Kingdom

¹¹Budker Institute of Nuclear Physics, Novosibirsk 630090, Russia

¹²University of California at Irvine, Irvine, CA 92697, USA

¹³University of California at Los Angeles, Los Angeles, CA 90024, USA

¹⁴University of California at San Diego, La Jolla, CA 92093, USA

¹⁵University of California at Santa Barbara, Santa Barbara, CA 93106, USA

¹⁶University of California at Santa Cruz, Institute for Particle Physics, Santa Cruz, CA 95064, USA

¹⁷California Institute of Technology, Pasadena, CA 91125, USA

¹⁸University of Cincinnati, Cincinnati, OH 45221, USA

¹⁹University of Colorado, Boulder, CO 80309, USA

²⁰Colorado State University, Fort Collins, CO 80523, USA

²¹Technische Universität Dresden, Institut für Kern- und Teilchenphysik, D-01062 Dresden, Germany

²²Ecole Polytechnique, LLR, F-91128 Palaiseau, France

- ²³University of Edinburgh, Edinburgh EH9 3JZ, United Kingdom
²⁴Università di Ferrara, Dipartimento di Fisica and INFN, I-44100 Ferrara, Italy
²⁵Florida A&M University, Tallahassee, FL 32307, USA
²⁶Laboratori Nazionali di Frascati dell'INFN, I-00044 Frascati, Italy
²⁷Università di Genova, Dipartimento di Fisica and INFN, I-16146 Genova, Italy
²⁸Harvard University, Cambridge, MA 02138, USA
²⁹University of Iowa, Iowa City, IA 52242, USA
³⁰Iowa State University, Ames, IA 50011-3160, USA
³¹Laboratoire de l'Accélérateur Linéaire, F-91898 Orsay, France
³²Lawrence Livermore National Laboratory, Livermore, CA 94550, USA
³³University of Liverpool, Liverpool L69 3BX, United Kingdom
³⁴University of London, Imperial College, London, SW7 2BW, United Kingdom
³⁵Queen Mary, University of London, E1 4NS, United Kingdom
³⁶University of London, Royal Holloway and Bedford New College, Egham, Surrey TW20 0EX, United Kingdom
³⁷University of Louisville, Louisville, KY 40292, USA
³⁸University of Manchester, Manchester M13 9PL, United Kingdom
³⁹University of Maryland, College Park, MD 20742, USA
⁴⁰University of Massachusetts, Amherst, MA 01003, USA
⁴¹Massachusetts Institute of Technology, Laboratory for Nuclear Science, Cambridge, MA 02139, USA
⁴²McGill University, Montréal, QC, Canada H3A 2T8
⁴³Università di Milano, Dipartimento di Fisica and INFN, I-20133 Milano, Italy
⁴⁴University of Mississippi, University, MS 38677, USA
⁴⁵Université de Montréal, Laboratoire René J. A. Lévesque, Montréal, QC, Canada H3C 3J7
⁴⁶Mount Holyoke College, South Hadley, MA 01075, USA
⁴⁷Università di Napoli Federico II, Dipartimento di Scienze Fisiche and INFN, I-80126, Napoli, Italy
⁴⁸NIKHEF, National Institute for Nuclear Physics and High Energy Physics, 1009 DB Amsterdam, The Netherlands
⁴⁹University of Notre Dame, Notre Dame, IN 46556, USA
⁵⁰Oak Ridge National Laboratory, Oak Ridge, TN 37831, USA
⁵¹Ohio State University, Columbus, OH 43210, USA
⁵²University of Oregon, Eugene, OR 97403, USA
⁵³Università di Padova, Dipartimento di Fisica and INFN, I-35131 Padova, Italy
⁵⁴Universités Paris VI et VII, Lab de Physique Nucléaire H. E., F-75252 Paris, France
⁵⁵Università di Pavia, Dipartimento di Elettronica and INFN, I-27100 Pavia, Italy
⁵⁶University of Pennsylvania, Philadelphia, PA 19104, USA
⁵⁷Università di Pisa, Dipartimento di Fisica, Scuola Normale Superiore and INFN, I-56127 Pisa, Italy
⁵⁸Prairie View A&M University, Prairie View, TX 77446, USA
⁵⁹Princeton University, Princeton, NJ 08544, USA
⁶⁰Università di Roma La Sapienza, Dipartimento di Fisica and INFN, I-00185 Roma, Italy
⁶¹Universität Rostock, D-18051 Rostock, Germany
⁶²Rutherford Appleton Laboratory, Chilton, Didcot, Oxon, OX11 0QX, United Kingdom
⁶³DAPNIA, Commissariat à l'Energie Atomique/Saclay, F-91191 Gif-sur-Yvette, France
⁶⁴University of South Carolina, Columbia, SC 29208, USA
⁶⁵Stanford Linear Accelerator Center, Stanford, CA 94309, USA
⁶⁶Stanford University, Stanford, CA 94305-4060, USA
⁶⁷State Univ. of New York, Albany, NY 12222, USA
⁶⁸University of Tennessee, Knoxville, TN 37996, USA
⁶⁹University of Texas at Austin, Austin, TX 78712, USA
⁷⁰University of Texas at Dallas, Richardson, TX 75083, USA
⁷¹Università di Torino, Dipartimento di Fisica Sperimentale and INFN, I-10125 Torino, Italy
⁷²Università di Trieste, Dipartimento di Fisica and INFN, I-34127 Trieste, Italy
⁷³Vanderbilt University, Nashville, TN 37235, USA
⁷⁴University of Victoria, Victoria, BC, Canada V8W 3P6
⁷⁵University of Wisconsin, Madison, WI 53706, USA
⁷⁶Yale University, New Haven, CT 06511, USA

(Dated: July 29, 2003)

We present measurements of branching fractions and charge asymmetries for charmless B -meson decays to three-body final states of charged pions and kaons. The analysis uses 81.8 fb^{-1} of data collected at the $\Upsilon(4S)$ resonance with the BABAR detector at the SLAC PEP-II asymmetric B Factory. We measure the branching fractions $\mathcal{B}(B^+ \rightarrow \pi^+ \pi^- \pi^+) = (10.9 \pm 3.3 \pm 1.6) \times 10^{-6}$, $\mathcal{B}(B^+ \rightarrow K^+ \pi^- \pi^+) = (59.1 \pm 3.8 \pm 3.2) \times 10^{-6}$, and $\mathcal{B}(B^+ \rightarrow K^+ K^- K^+) = (29.6 \pm 2.1 \pm 1.6) \times 10^{-6}$, and provide 90% C.L. upper limits for other decays. We observe no charge asymmetries for these modes.

The study of charmless hadronic B decays can make important contributions to the understanding of CP violation in the Standard Model, as well as to models of hadronic decays. Reference [1] proposes that the interference between various charmless decays and the χ_{c0} resonance can be used to measure the Cabibbo-Kobayashi-Maskawa (CKM) angle γ , while the decay $B^+ \rightarrow \pi^+\pi^-\pi^+$ can be used to reduce the uncertainties in the measurement of the CKM angle α [2]. We present branching fractions and charge asymmetries of charged- B -meson decays to three-body final states of charged pions and kaons [3], with no assumptions about intermediate resonances and with charm contributions subtracted, which allows us to set a tight bound on the charmless contribution to the measurement of γ [1]. Upper limits and measurements of some of these branching fractions have been obtained previously with smaller statistics [4].

The data used in this analysis were collected at the PEP-II asymmetric e^+e^- storage ring with the *BABAR* detector, described in detail elsewhere [5]. The on-resonance data sample consists of 88.8 million $B\bar{B}$ pairs collected at the $\Upsilon(4S)$ resonance during the years 1999–2002. We also use 9.6 fb^{-1} of off-resonance data, collected 40 MeV below the $\Upsilon(4S)$ resonance, to characterize the backgrounds from e^+e^- annihilation into light $q\bar{q}$ pairs. We assume that the $\Upsilon(4S)$ decays equally to neutral and charged B meson pairs.

Hadronic events are selected based on track multiplicity and event topology. Backgrounds from non-hadronic events are reduced by requiring the ratio of Fox-Wolfram moments H_2/H_0 [6] to be less than 0.98. Candidate B decays are formed by combining three charged tracks, where each track is required to have at least 12 hits in the tracking chamber, a minimum transverse momentum of 100 MeV/ c , and to be consistent with originating from the beam-spot.

Signal decays are identified using two kinematic variables: 1) the difference ΔE between the center-of-mass (CM) energy of the B candidate and $\sqrt{s}/2$, where \sqrt{s} is the total CM energy, and 2) the beam-energy substituted mass $m_{\text{ES}} = \sqrt{(s/2 + \mathbf{p}_i \cdot \mathbf{p}_B)^2/E_i^2 - \mathbf{p}_B^2}$, where the B momentum \mathbf{p}_B and the four-momentum of the initial state (E_i, \mathbf{p}_i) are defined in the laboratory frame. The ΔE and m_{ES} distributions of signal events are Gaussian with resolutions of 20 MeV and 2.7 MeV/ c^2 , respectively. The typical ΔE separation between modes that differ by substituting a kaon for a pion in the final state is 45 MeV, assuming the pion mass hypothesis.

Charged pions and kaons are identified using energy loss (dE/dx) in the silicon detector and tracking chamber, and, for tracks with momenta above 700 MeV/ c , the Cherenkov angle and number of photons measured by the Cherenkov detector. The efficiency of selecting kaons is

approximately 80%, which includes the geometrical acceptance, while the probability of misidentifying pions as kaons is below 5%, up to a laboratory momentum of 4.0 GeV/ c . Pions are required to fail both the kaon selection and an electron selection algorithm based on information from dE/dx , shower shapes in the calorimeter and the ratio of the shower energy and track momentum.

We remove B candidates when the invariant mass of the combination of any two of its daughter tracks (of opposite charge) is within 6σ of the mass of the D^0 meson or within 3σ of the mass of the J/ψ , $\psi(2S)$ or χ_{c0} mesons [7]. Here, σ is 10 MeV/ c^2 for D^0 , 15 MeV/ c^2 for J/ψ and $\psi(2S)$, and 18 MeV/ c^2 for χ_{c0} .

To suppress background from light-quark and charm continuum production, two event-shape variables are computed in the CM frame. The first is the cosine of the angle θ_T^* between the thrust axis of the selected B candidate and the thrust axis of the rest of the event, i.e. all charged tracks and neutral particles not assigned to the B candidate. For jet-like continuum backgrounds, $|\cos\theta_T^*|$ is strongly peaked towards unity, while it is essentially uniform for signal events. For each signal mode we fix an upper limit on $|\cos\theta_T^*|$, between 0.575 and 0.850. This rejects between 95% and 85% of the background, depending on the decay mode.

The second event-shape variable is a Fisher discriminant [8], which is formed from the summed scalar momenta of all charged and neutral particles from the rest of the event within nine 10° -wide nested cones coaxial with the thrust axis of the B candidate. The coefficients of the Fisher discriminant are chosen to maximize the separation between signal and continuum background events, and are calculated for each signal mode separately using Monte Carlo simulated signal and continuum events. A further 50% to 75% of the remaining background is rejected, depending on the decay mode, by applying selection requirements on this variable.

B decay candidates passing the above selection criteria are required to lie in a signal region defined as follows: $|m_{\text{ES}} - m_B| < 8 \text{ MeV}/c^2$ and $|\Delta E - \langle\Delta E\rangle| < 60 \text{ MeV}$, where $\langle\Delta E\rangle = 7 \text{ MeV}$ is the mean value of ΔE measured from on-resonance data for the calibration sample $B^- \rightarrow D^0\pi^-$, $D^0 \rightarrow K^-\pi^+$, and m_B is the nominal mass of the charged B meson [7]. Figure 1 shows the projections of the on-resonance data in the signal region onto the ΔE and m_{ES} axes. Each plot shows the expected levels of continuum and $B\bar{B}$ background, where the latter is parameterized from Monte Carlo samples.

The residual continuum background level is estimated from the observed number of events in the grand sideband (GSB) region, defined to be $5.21 < m_{\text{ES}} < 5.25 \text{ GeV}/c^2$ and $|\Delta E - \langle\Delta E\rangle| < 100 \text{ MeV}$, and extrapolating into the signal region. The shape of the m_{ES} distribution of

the background is parameterized according to the phenomenologically motivated ARGUS function [9], and is measured using off-resonance data and the upper sideband in the ΔE variable in on-resonance data ($0.10 < \Delta E < 0.25$ GeV). A quadratic function is used to parameterize the ΔE distribution of the background. The ratio of the integrals over the signal and GSB regions of the product of the ΔE and m_{ES} shape functions, R , gives the ratio of the number of background events in the two areas.

The branching fraction for each channel is measured over the whole Dalitz plot, which is divided into 28×28 cells of equal area ($1 \text{ GeV}^2/c^4)^2$ to enable us to find the selection efficiency as a function of position in the Dalitz plot. Taking ϵ_i to be the efficiency of reconstructing the signal in the i^{th} bin of the Dalitz plot, determined from Monte Carlo simulated events, the branching fraction for each signal mode is given by:

$$\mathcal{B} = \frac{1}{N_{B\bar{B}}} \left(\sum_i \frac{(N_{1i} - RN_{2i} - N_x p_i)}{\epsilon_i} - n_x - n_b \right), \quad (1)$$

where N_{1i} and N_{2i} are the number of events observed in the signal and GSB regions, respectively, while $N_x p_i$, n_x and n_b are background contributions that are defined below. $N_{B\bar{B}}$ is the total number of $B\bar{B}$ pairs in the data sample. No significant differences were found for the value of R (defined earlier) in different regions of the Dalitz plot, so an average value is used for all bins.

The probability of a kaon being misidentified as a pion is 20%. This means there is significant cross-feed into the signal region from the decay mode that has one more kaon, which is subtracted for each bin, i . This is represented by the $N_x p_i/\epsilon_i$ term in Eq. (1), where N_x is the total number of events that is the source of the cross-feed, and p_i is the probability for the cross-feed events to pass the selection criteria for the i^{th} bin, which is estimated from Monte Carlo samples. The $B^+ \rightarrow K^+ K^- K^+$ mode has $N_x = 0$, since it has no cross-feed backgrounds. For the other decays, N_x is obtained by multiplying $N_{B\bar{B}}$ by the branching fraction of the signal mode that has a kaon substituting a pion in the final state. There is also second-order cross-feed where either two kaons are misidentified as pions (probability of 4%), or one of the pions is misidentified as a kaon (probability of 2%). This is represented by the n_x term in Eq. (1).

Finally, the n_b term represents the small number of other $B\bar{B}$ backgrounds that are subtracted. For all signal modes except $B^+ \rightarrow K^+ K^- K^+$, n_b is obtained from the number of D^0 and \bar{D}^0 candidates whose invariant mass is beyond the 6σ range. For $B^+ \rightarrow K^+ \pi^- \pi^+$, there is also a contribution from $B^\pm \rightarrow \eta'(\rightarrow \rho^0 \gamma) K^\pm$ decays, which is estimated from the selection efficiency from Monte Carlo simulated decays, and the branching fraction quoted in Ref. [7]. By using a mixture of Monte-Carlo-simulated charm and charmless decays, we found that there were

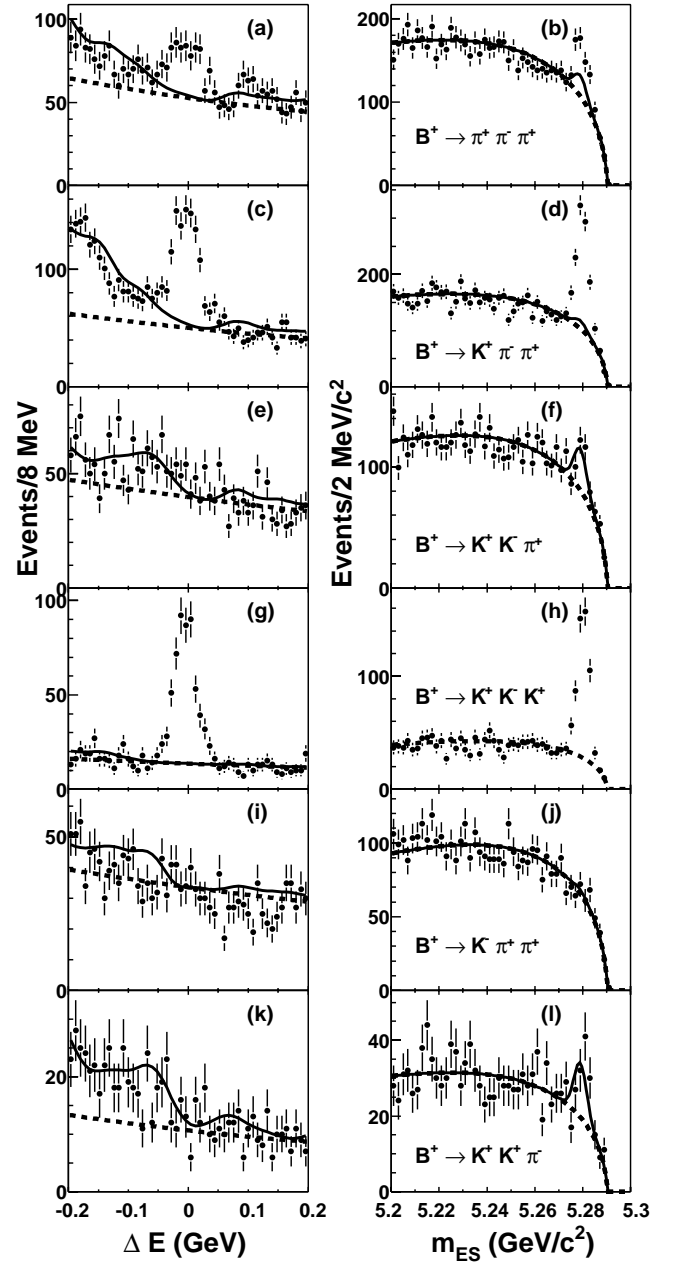


FIG. 1: Projections of ΔE and m_{ES} for $B^+ \rightarrow \pi^+ \pi^- \pi^+$ (a and b), $B^+ \rightarrow K^+ \pi^- \pi^+$ (c and d), $B^+ \rightarrow K^+ K^- \pi^+$ (e and f), $B^+ \rightarrow K^+ K^- K^+$ (g and h), $B^+ \rightarrow K^- \pi^+ \pi^+$ (i and j) and $B^+ \rightarrow K^+ K^+ \pi^-$ (k and l) in the signal region. The signal region requirement was made on the orthogonal variable in each case. The dashed curves show the continuum background, while the solid lines include the $B\bar{B}$ background.

no other significant $B\bar{B}$ backgrounds.

We do not divide the Dalitz plot into cells for the Standard-Model-suppressed modes $B^+ \rightarrow K^- \pi^+ \pi^+$ and $B^+ \rightarrow K^+ K^+ \pi^-$, and instead use the average values of the signal efficiency and cross-feed terms.

The branching fraction results are summarized in Ta-

TABLE I: Branching fraction results for on-resonance data. The quantities and their uncertainties are explained in the text.

Signal Mode	$\pi^\pm\pi^\mp\pi^\pm$	$K^\pm\pi^\mp\pi^\pm$	$K^\pm K^\mp\pi^\pm$	$K^\pm K^\mp K^\pm$	$K^\mp\pi^\pm\pi^\pm$	$K^\pm K^\pm\pi^\mp$
$\sum_i N_{1i}$	1029	1502	733	646	494	209
$\sum_i N_{2i}$	5577	5209	4012	1308	3268	1025
$\langle \epsilon \rangle (\%)$	12.7 ± 0.5	12.8 ± 1.4	13.9 ± 0.9	14.9 ± 0.9	18.5 ± 0.9	15.3 ± 0.7
R	0.144 ± 0.003	0.146 ± 0.003	0.150 ± 0.003	0.158 ± 0.006	0.155 ± 0.003	0.157 ± 0.006
A) $\sum_i N_{1i}/\epsilon_i$	7597 ± 275	11056 ± 327	5071 ± 216	4011 ± 182	2670 ± 120	1366 ± 94
B) $\sum_i RN_{2i}/\epsilon_i$	$5938 \pm 94 \pm 117$	$5604 \pm 89 \pm 111$	$4041 \pm 72 \pm 80$	$1381 \pm 46 \pm 55$	$2738 \pm 48 \pm 53$	$1052 \pm 33 \pm 40$
C) $\sum_i N_x p_i/\epsilon_i$	$474 \pm 33 \pm 40$	$22 \pm 1 \pm 30$	$671 \pm 15 \pm 59$	—	—	344 ± 31
D) n_x	—	-189 ± 34	110 ± 128	—	—	53 ± 5
E) D^0 Bkgnd	216 ± 24	268 ± 28	47 ± 6	—	33 ± 5	31 ± 5
F) $\eta'K$ Bkgnd	—	106 ± 30	—	—	—	—
G) Signal Yield	$970 \pm 291 \pm 130$	$5246 \pm 339 \pm 127$	$202 \pm 227 \pm 163$	$2630 \pm 188 \pm 55$	$-101 \pm 129 \pm 53$	$-114 \pm 100 \pm 51$
	$\pm 22 \pm 50$	$\pm 39 \pm 247$	$\pm 16 \pm 9$	$\pm 12 \pm 124$	$\pm 0 \pm 5$	$\pm 0 \pm 5$
$\mathcal{B} (\times 10^{-6})$	$10.9 \pm 3.3 \pm 1.6$	$59.1 \pm 3.8 \pm 3.2$	$2.3 \pm 2.6 \pm 1.8$	$29.6 \pm 2.1 \pm 1.6$	$-1.1 \pm 1.5 \pm 0.6$	$-1.3 \pm 1.1 \pm 0.6$
Significance (σ)	5.7	> 6	1.1	> 6	—	—
90% C.L.	—	—	< 6.3	—	< 1.8	< 1.3

ble I, where the first four rows show the total number of events in the signal and GSB regions, the average signal efficiencies $\langle \epsilon \rangle$, and the values of R for each mode. The absolute efficiency variation across the Dalitz plot typically varies between $\pm 2\%$ and $\pm 5\%$ from $\langle \epsilon \rangle$.

Rows A and B represent the total number of events and the amount of continuum background in the signal region, corrected for efficiency. The uncertainties for row A come from the statistical errors in N_{1i} , while the uncertainties for row B correspond to the statistical errors in N_{2i} , and the systematic errors from R , which arise from the limited statistics in the sideband region and off-resonance data.

Row C shows the expected background from cross-feed events. The first and second uncertainties of these quantities represent the systematic errors in p_i and N_x , respectively, except for the channel $B^+ \rightarrow K^+ K^+ \pi^-$, where the uncertainty represents the average of the p_i and N_x contributions. The second-order cross-feed terms n_x are shown in row D. Note that the n_x term for $B^+ \rightarrow K^+ \pi^- \pi^+$ is negative, which corrects for the $B^+ \rightarrow K^+ K^- K^+$ cross-feed into $B^+ \rightarrow K^+ K^- \pi^+$, which in turn contributes to the cross-feed background for $B^+ \rightarrow K^+ \pi^- \pi^+$.

Rows E and F show the expected backgrounds from D^0 and $\eta'K$ decays, which include the uncertainties from the selection efficiencies and the branching fractions of the background decays [7]. The sum of these two rows gives the value of n_b in Eq. (1).

Row G shows the signal yield, obtained by subtracting rows B to F from row A. The first uncertainty is the combination of the statistical errors of the number of events in the signal and GSB regions. The second uncertainty corresponds to the sum in quadrature of all the systematic errors from rows B to F. The third error is from the bin-by-bin uncertainty of the selection efficiency.

This is zero for $B^+ \rightarrow K^- \pi^+ \pi^+$ and $B^+ \rightarrow K^+ K^+ \pi^-$, where we only use the average efficiencies. The last uncertainty originates from global systematic errors in the signal efficiencies due to charged-particle tracking (0.8% per track), event-shape variable selections (1.0 to 2.5%) and from particle identification (1.4% and 1.0% per pion and kaon track, respectively).

The next row in Table I shows the branching fraction results, where the first uncertainties are from the statistical errors in the number of events, while the second uncertainties are the sum in quadrature of all systematic errors mentioned above.

The significance of each branching fraction result, under the null hypothesis, is defined as the ratio of the signal yield to the total (statistical and systematic) uncertainty of the background in the signal region. We observe significant signals for the modes $B^+ \rightarrow \pi^+ \pi^- \pi^+$, $B^+ \rightarrow K^+ \pi^- \pi^+$ and $B^+ \rightarrow K^+ K^- K^+$, and provide 90% C.L. upper limits for the other channels, using the formalism in Ref. [10]. The branching fraction of the control sample $B^- \rightarrow D^0 \pi^-$, $D^0 \rightarrow K^- \pi^+$, which has the same final state as $B^+ \rightarrow K^+ \pi^- \pi^+$, is measured to be $(190 \pm 3 \pm 10) \times 10^{-6}$, which agrees with the average of published measurements $(201 \pm 20) \times 10^{-6}$ [7].

We have also measured the charge asymmetries for the modes with observed signals using a method similar to that used for the branching fraction measurements. The charge asymmetries are defined as $\mathcal{A} = (N^- - N^+) / (N^- + N^+)$, where N^- (N^+) is the signal yield for negatively (positively) charged B candidates, as defined by row G in Table I. The normalisation factor $N_{B\bar{B}}$ cancels out in the asymmetry ratio, while the cross-feed and $B\bar{B}$ background contributions cancel in the asymmetry numerator. The measured charge asymmetries are $\mathcal{A}(B^+ \rightarrow \pi^+ \pi^- \pi^+) = -0.39 \pm 0.33 \pm 0.12$, $\mathcal{A}(B^+ \rightarrow K^+ \pi^- \pi^+) = 0.01 \pm 0.07 \pm 0.03$ and $\mathcal{A}(B^+ \rightarrow$

$K^+K^-K^+)$ = $0.02 \pm 0.07 \pm 0.03$, where the first uncertainties are statistical and the second are systematic, which include the charge bias of the tracking and particle identification selection requirements (1%).

In summary, we have measured the branching fraction of $B^+ \rightarrow \pi^+\pi^-\pi^+$ for the first time, which is smaller than that assumed in Ref. [1], and we have also observed the channels $B^+ \rightarrow K^+\pi^-\pi^+$ and $B^+ \rightarrow K^+K^-K^+$. We observed no charge asymmetries in these decays.

We are grateful for the excellent luminosity and machine conditions provided by our PEP-II colleagues, and for the substantial dedicated effort from the computing organizations that support *BABAR*. The collaborating institutions wish to thank SLAC for its support and kind hospitality. This work is supported by DOE and NSF (USA), NSERC (Canada), IHEP (China), CEA and CNRS-IN2P3 (France), BMBF and DFG (Germany), INFN (Italy), FOM (The Netherlands), NFR (Norway), MIST (Russia), and PPARC (United Kingdom). Individuals have received support from the A. P. Sloan Foundation, Research Corporation, and Alexander von Humboldt Foundation.

- [†] Also with Università della Basilicata, Potenza, Italy
- [‡] Also with IFIC, Instituto de Física Corpuscular, CSIC-Universidad de Valencia, Valencia, Spain
- [§] Deceased
- [1] B. Bajc *et al.*, Phys. Lett. B **447**, 313 (1999).
- [2] A.E. Snyder, H.R. Quinn, Phys. Rev. D **48**, 2139 (1993).
- [3] Throughout this paper, flavor-eigenstate decay modes imply also their charge conjugate.
- [4] CLEO Collaboration, T. Bergfeld *et al.*, Phys. Rev. Lett. **77**, 4503 (1996); BELLE Collaboration, A. Garmash *et al.*, Phys. Rev. D **65**, 092005 (2002).
- [5] BABAR Collaboration, B. Aubert *et al.*, Nucl. Instr. and Meth. A **479**, 1 (2002).
- [6] G.C. Fox and S. Wolfram, Phys. Rev. Lett. **41**, 1581 (1978).
- [7] Particle Data Group, K. Hagiwara *et al.*, Phys. Rev. D **66**, 010001 (2002).
- [8] CLEO Collaboration, D.M. Asner *et al.*, Phys. Rev. D **53**, 1039 (1996).
- [9] ARGUS Collaboration, H. Albrecht *et al.*, Z. Phys. C **48**, 543 (1990).
- [10] G.J. Feldman and R.D. Cousins, Phys. Rev. D **57**, 3873 (1998).

* Also with Università di Perugia, Perugia, Italy